

Thermal Conductivity of Opacified Powder Filler Materials for Vacuum Insulations¹

R. Caps^{2,3} and J. Fricke²

The thermal conductivity of powder fillings for load-bearing vacuum insulations is investigated. Different opacifiers have been tested in mixtures with perlite powder, precipitated silica, and fumed silica. Using temperature-dependent thermal conductivity measurements, the radiative thermal conductivity and the solid conductivity of the powder samples are separated. Additionally, the influence of the pressure load on the solid conductivity is studied. The thermal conductivities of silica powders with added opacifier powders (carbon black, magnetite, silicon carbide, titanium dioxide) can be as low as $0.003 \text{ W} \cdot \text{m}^{-1} \cdot \text{K}^{-1}$ if the powder boards are pressed with moderate loads. The use of microporous silica powders as filler materials allows internal gas pressures even beyond 10 hPa with only a moderate increase of the overall conductivity.

KEY WORDS: evacuated insulations; opacifier; powders; radiative conductivity; silica powder; silicon carbide; thermal conductivity; thermal radiation.

1. INTRODUCTION

Load-bearing evacuated insulations provide up to 10-fold lower thermal conductivity compared to conventional, air-filled insulation materials. They may be used for the efficient insulation of refrigerators, cold stores, refrigerator trucks, and even building facades. Many systems currently are under development and some are also commercially available. Filler materials for the vacuum insulations may be glass fibers [1], open pore organic foams [2, 3], and powders [4, 5].

¹ Paper presented at the Fifth Asian Thermophysical Properties Conference, August 30–September 2, 1998, Seoul, South Korea.

² Bavarian Center for Applied Energy Research (ZAE Bayern), Am Hubland, D-97074 Würzburg, Germany.

³ To whom correspondence should be addressed.

The construction of the cover of the evacuated panels depends on the maximum allowable gas pressure which does not increase the thermal conductivity significantly. For glass fibers, welded stainless steel foil packages are necessary, which keep the internal gas pressure below 0.1 hPa during the time of use. Organic foams may be wrapped with laminated aluminum foils combined with a suitable getter material, which keeps the gas pressure below 1 hPa. High-barrier plastic foils without any metal layer may be used if the maximum allowable gas pressure is in the range of 10–20 hPa. This relatively large pressure is possible if microporous powders are used as filler material; they additionally have considerable capacity to adsorb water vapor diffusing through the envelope.

The ZAE Bayern has developed vacuum panels which are covered by glass panes on both sides. They can be used as highly insulating facade elements in connection with transparent window elements [6]. The rim construction of the panel has to be made in such a way that thermal bridging is avoided, and the panel is sufficiently vacuum-tight in order to provide lifetimes beyond 20 years. One solution of the rim is shown in Fig. 1. A high-barrier plastic foil is connected to the glass panes by adhesives. As the increase of gas pressure due to the diffusion of air through the plastic foil and the adhesive layer cannot be suppressed to less than 1 hPa per year, this construction is only suitable if microporous filler materials are used.

As part of the above development, different microporous powders have been investigated in order to optimize thermal performance. We have measured the thermal conductivity of mixtures of perlite powders, precipitated and fumed silica powders, and different opacifier powders. Using these data, we analyzed the different heat transfer contributions of the various powders, and used the results for further optimization.

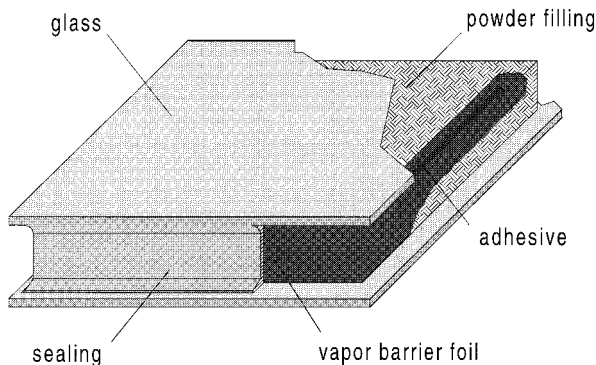


Fig. 1. Sketch of glass-covered vacuum panel.

2. MEASUREMENTS AND ANALYSIS

The thermal conductivity measurements have been performed with an evacuable guarded hot plate device. The samples (diameter 200 mm) were pressed with an external mechanical load between 0.01 and 0.4 MPa. The mean temperature T was varied between 10 and 400°C. From the temperature dependence of the thermal conductivity, the radiative conductivity and the thermal radiation extinction coefficient E are derived by fitting the data to an appropriate model for the thermal conductivity λ :

$$\lambda(p_{\text{gas}} = 0) = \lambda_s(T) + \frac{16}{3} \frac{n^2 \sigma T^3}{E(T)} \quad (1)$$

The temperature dependence of the solid conductivity λ_s of silica-based powders was usually assumed to be proportional to the known temperature dependent thermal conductivity of silica glass. If an opacifier powder is used as an additive, the temperature dependence of the extinction coefficient E in most cases can be neglected and it can be taken as a constant.

The increase of thermal conductivity with the rise of the internal gas pressure generally can be described by

$$\lambda(p_{\text{gas}}) = \lambda(p_{\text{gas}} = 0) + \frac{\lambda_{\text{gas}}^0}{1 + (p_{1/2}/p_{\text{gas}})} \quad (2)$$

This equation is a good approximation, especially for $p < p_{1/2}$.

In Table I the properties of the measured powders and powder mixtures are compiled.

3. RESULTS

As an example of the analysis, the thermal conductivity of a mixture of precipitated silica with silicon carbide powder, sample SICSIP28, is presented. First, the evacuated powder sample was loaded at pressures between 0.01 and 0.16 MPa and the thermal conductivity measured. Then the temperature variation of the thermal conductivity was determined at a pressure load of 0.1 MPa (see Fig. 2).

At room temperature the thermal conductivity of this sample is around $0.003 \text{ W} \cdot \text{m}^{-1} \cdot \text{K}^{-1}$, which is about $0.002\text{--}0.003 \text{ W} \cdot \text{m}^{-1} \cdot \text{K}^{-1}$ lower than for pure precipitated silica. At a mean temperature of 250°C, the thermal conductivity increases to $0.006 \text{ W} \cdot \text{m}^{-1} \cdot \text{K}^{-1}$.

Applying Eq. (1) to the data, we obtain an extinction coefficient $E = 14000 \text{ m}^{-1}$. The specific extinction $e = E/\rho$ is $61 \text{ m}^2 \cdot \text{kg}^{-1}$ with density $\rho = 232 \text{ kg} \cdot \text{m}^{-3}$ (at 0.1 MPa external load).

Table I. Properties of Samples

Sample	Contents ^a	ρ ($\text{kg} \cdot \text{m}^{-3}$)	E (m^{-1})	e ($\text{m}^2 \cdot \text{kg}^{-1}$)	$p_{1/2}$ (hPa)
PERL	100% perlite	219	—	—	5
PAFLA	+10% c.b. +10% p.SiO ₂	220	11300	51	20
FEPESIP	+20% Fe ₃ O ₄ +40% f.SiO ₂	306	15400	50	150
SIP	100% p.SiO ₂	180	3600	20	220
ILSIP28	+20% FeTiO ₃	213	6500	30	200
RUSIP19	+10% c.b.	182	10600	58	190
FESIP28	+20% Fe ₃ O ₄	202	10300	51	—
FESIP37	+30% Fe ₃ O ₄	253	26000	104	200
SICSIP28	+20% SiC	232	14000	61	—
MICRO	70% f.SiO ₂ +30% TiO ₂	~240	14700	61	590
AP01	90% SiO ₂ -aerogel +10% c.b.	166	8100	49	4/530 ^b

^a c.b., carbon black; p.SiO₂, precipitated silica; f.SiO₂, fumed silica.

^b Bimodal distribution of pores within and between the powder granules.

The solid conductivity $\lambda_s(T)$ is also obtained by the above fitting procedure (see Fig. 2). At room temperature it amounts to about $0.002 \text{ W} \cdot \text{m}^{-1} \cdot \text{K}^{-1}$ and is slightly increasing with temperature. The corresponding radiative conductivity is less than $0.001 \text{ W} \cdot \text{m}^{-1} \cdot \text{K}^{-1}$ at room temperature and increases to about $0.003 \text{ W} \cdot \text{m}^{-1} \cdot \text{K}^{-1}$ at 250°C .

In a further step the sample was reloaded with external loads of up to 0.4 MPa at room temperature. At a pressure load $p_{\text{ext}} = 0.4 \text{ MPa}$, according

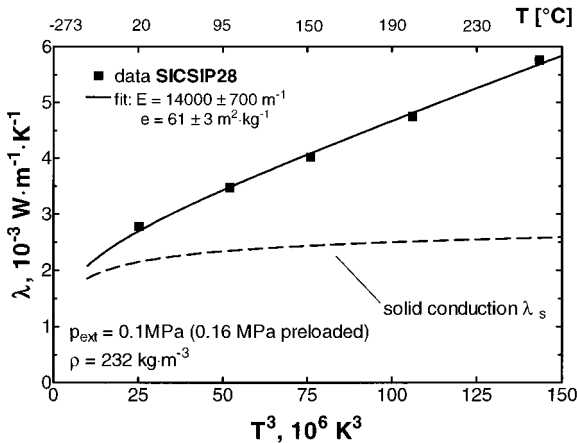


Fig. 2. Thermal conductivity λ of sample SICSIP28 as a function of T^3 .

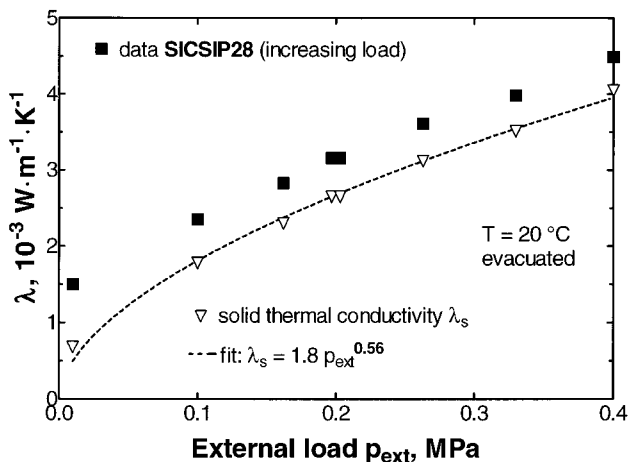


Fig. 3. Thermal conductivity λ of sample SICSIP28 as a function of external load p_{ext} .

to Fig. 3, the thermal conductivity of the sample increases to $0.0045 \text{ W} \cdot \text{m}^{-1} \cdot \text{K}^{-1}$. When the radiative conductivity is subtracted from such data, the solid conductivity as a function of the pressure load p_{ext} is obtained. As can be seen in Fig. 3, it varies proportional to $p_{\text{ext}}^{0.56}$.

In the same way the solid conductivity λ_s of the other samples has been analyzed. A summary of the results is shown in Fig. 4. All samples based on perlite powders reveal a solid conductivity which is considerably

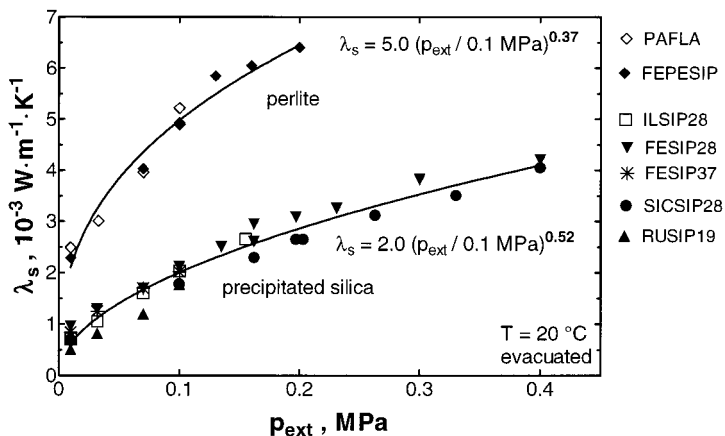


Fig. 4. Solid thermal conductivity λ_s of samples based on perlite and precipitated silica as a function of external load p_{ext} .

higher than the solid conductivity of the samples based on precipitated silica. At 0.1 MPa external load the perlite powders reach $\lambda_s = 0.005 \text{ W} \cdot \text{m}^{-1} \cdot \text{K}^{-1}$, whereas the solid conductivity of the silica based powders is just $\lambda_s = 0.002 \text{ W} \cdot \text{m}^{-1} \cdot \text{K}^{-1}$. The increase of the solid conductivity with external load for the silica powders is approximately proportional to the square root of p_{ext} and nearly independent of the kind of opacifier.

The change of thermal conductivity with gas pressure for samples based on perlite (FEPESIP), precipitated silica (FESIP37), fumed silica (MICRO), and aerogel powder (AP01) [7] is depicted in Fig. 5 for comparison. At low gas pressures the lowest thermal conductivity is obtained by the FESIP37 sample, which had been opacified with 30% iron oxide, Fe_3O_4 . The thermal conductivity of a pressed board made from fumed silica with 30% TiO_2 powder as opacifier is somewhat higher at low gas pressures, but yields the lowest increase with rising gas pressure. Even at 1000 hPa atmospheric gas pressure, the thermal conductivity is just around $0.020 \text{ W} \cdot \text{m}^{-1} \cdot \text{K}^{-1}$. The gas conductivity of the aerogel powder AP01 starts to increase considerably, even at gas pressures of 1 hPa, and thus cannot be used for the glass-covered vacuum panels as discussed in the Introduction. The thermal conductivity of perlite-based sample FEPESIP is rather high; at 10 hPa it is beyond $0.008 \text{ W} \cdot \text{m}^{-1} \cdot \text{K}^{-1}$.

Table I gives the characteristic gas pressures $p_{1/2}$ of the samples as derived from the gas pressure-dependent measurements according to Eq. (2). The characteristic gas pressure $p_{1/2}$ is inversely proportional to the mean pore size and thus also related to the dimension of the powder particles. The highest characteristic gas pressure is obtained for the microporous silica

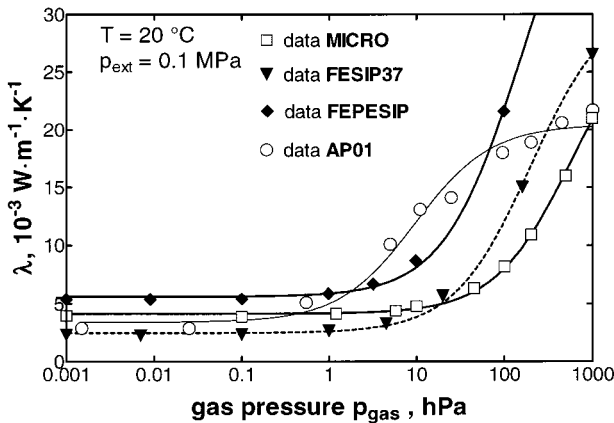


Fig. 5. Thermal conductivity λ as a function of gas pressure p_{gas} ; the lines are fits according to Eq. (2).

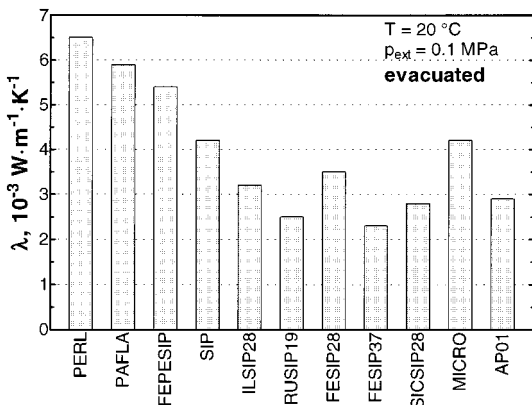


Fig. 6. Comparison of thermal conductivity λ of the evacuated samples ($p_{\text{gas}} < 10^{-2}$ hPa) at room temperature.

powder MICRO with $p_{1/2} = 600$ hPa, whereas the value for precipitated silica is in the range of 200 hPa and the pure perlite powder with grain sizes on the order of $10 \mu\text{m}$ has $p_{1/2} = 5$ hPa. The addition of opacifiers with powder particles in the range of some micrometers to precipitated or fumed silica usually does not influence the characteristic gas pressure $p_{1/2}$ significantly.

Figure 6 summarizes the measured thermal conductivities for fully evacuated specimens. Thermal conductivities as low as $0.003 \text{ W} \cdot \text{m}^{-1} \cdot \text{K}^{-1}$ are obtained in silica samples which have been opacified with carbon black (RUSIP19M), ilmenite (ILSIP28), iron oxide (FESIP37), and silicon carbide (SICSIP28). Note, however, that these samples were prepared with an external load of 0.1 MPa, except for SICSIP28, which was loaded with 0.16 MPa, and the Microtherm sample, which was pressed by the supplying company by an undetermined, considerably higher load (yielding a density of approximately $240 \text{ kg} \cdot \text{m}^{-3}$).

The highest specific extinction has been measured using 30% magnetite as opacifier (sample FESIP37 with $e = 100 \text{ m}^2 \cdot \text{kg}^{-1}$). The other samples had specific extinctions around $e = 50\text{--}60 \text{ m}^2 \cdot \text{kg}^{-1}$. Thus, the radiative conductivity could be suppressed to values below $0.001 \text{ W} \cdot \text{m}^{-1} \cdot \text{K}^{-1}$ at 300 K. It is remarkable that the 20% addition of silicon carbide powder to precipitated silica (sample SICSIP28) provided the same specific extinction as the sample MICRO, which contains 30% titanium dioxide powder as opacifier.

4. CONCLUSIONS

A combination of opacifier powders with either precipitated or fumed silica yields thermal conductivities around $0.003 \text{ W} \cdot \text{m}^{-1} \cdot \text{K}^{-1}$ if evacuated.

The maximum allowable internal gas pressure for a thermal conductivity below $0.005 \text{ W} \cdot \text{m}^{-1} \cdot \text{K}^{-1}$ is in the range of 10–20 hPa. If, additionally, the high adsorption capacity of dried silica powder for water vapor is taken into account, glass-covered vacuum panels (combined with high-barrier plastic rim foils) have lifetimes of considerably more than 20 years.

NOMENCLATURE

e	mass specific extinction	$[\text{m}^2 \cdot \text{kg}^{-1}]$
E	extinction coefficient	$[\text{m}^{-1}]$
n	effective index of refraction	
p_{ext}	external load	$[\text{MPa}]$
p_{gas}	gas pressure	$[\text{hPa}]$
$p_{1/2}$	characteristic gas pressure	$[\text{hPa}]$
T	mean temperature	$[\text{K}]$
λ	total conductivity	$[\text{W} \cdot \text{m}^{-1} \cdot \text{K}^{-1}]$
λ_s	solid conductivity	$[\text{W} \cdot \text{m}^{-1} \cdot \text{K}^{-1}]$
λ_r	radiative conductivity	$[\text{W} \cdot \text{m}^{-1} \cdot \text{K}^{-1}]$
λ_{gas}^0	thermal conductivity of free gas	$[\text{W} \cdot \text{m}^{-1} \cdot \text{K}^{-1}]$
σ	Stefan–Boltzmann constant	$5.67 \times 10^{-8} \text{ W} \cdot \text{m}^{-2} \cdot \text{K}^{-4}$
ρ	density	$[\text{kg} \cdot \text{m}^{-3}]$

ACKNOWLEDGMENTS

This work was funded by the German Ministry BMBF, Grant No. 0328654D. We thank Mr. Kloo from Microtherm Europe N.V., Belgium for providing us with fumed silica powder boards (sample MICRO).

REFERENCES

1. R. Caps, J. Hettfleisch, Th. Rettelbach, and J. Fricke, in *Thermal Conductivity 23*, K. E. Wilkes, R. B. Dinwiddie, and R. S. Graves, eds. (Technomic Publishing, Lancaster, Pennsylvania, 1996), pp. 373–382.
2. D. Rosbotham and R. De Vos, in *Proc. International Polyurethane Industry Conference Utech '94* (The Hague, Netherlands, 1994).
3. K. W. Dietrich and D. W. McCullough, in *Proc. International Polyurethane Industry Conference Utech '96* (The Hague, Netherlands, 1996).
4. R. Caps, Th. Rettelbach, M. Ehrmanntraut, S. Korder, and J. Fricke, in *Insulation Materials: Testing and Applications, Third Volume, ASTM STP 1320*, R. S. Graves and R. R. Zarr, eds. (American Society for Testing and Materials, 1997).
5. Th. Stovall, K. Wilkes, G. Nelson, and F. Weaver, in *Proc. 24th International Thermal Conductivity Conference* (Pittsburgh, Pennsylvania, 1997).
6. A. Beck, R. Caps, G. Gertner, and J. Fricke, in *Proc. 4th European Conference on Solar Energy in Architecture and Urban Planning* (Berlin, Germany, 1996).
7. E. Hümmer, X. Lu, Th. Rettelbach, and J. Fricke, *J. Non-Cryst. Solids* **145**:211 (1992).